

Discriminative Clustering with Relative Constraints

Yuanli Pei*, Xiaoli Z. Fern*, Rómer Rosales†, and Teresa Vania Tjahja*

*School of EECS, Oregon State University.

Email: {pei, xfern, tjahjat}@eecs.oregonstate.edu

†LinkedIn. Email: rrosales@linkedin.com

Abstract—We study the problem of clustering with *relative constraints*, where each constraint specifies relative similarities among instances. In particular, each constraint (x_i, x_j, x_k) is acquired by posing a query: *is instance x_i more similar to x_j than to x_k ?* We consider the scenario where answers to such queries are based on an underlying (but unknown) *class concept*, which we aim to discover via clustering. Different from most existing methods that only consider constraints derived from *yes* and *no* answers, we also incorporate *don't know* responses. We introduce a Discriminative Clustering method with Relative Constraints (DCRC) which assumes a natural probabilistic relationship between instances, their underlying cluster memberships, and the observed constraints. The objective is to maximize the model likelihood given the constraints, and in the meantime enforce cluster separation and cluster balance by also making use of the unlabeled instances. We evaluated the proposed method using constraints generated from ground-truth class labels, and from (noisy) human judgments from a user study. Experimental results demonstrate: 1) the usefulness of relative constraints, in particular when *don't know* answers are considered; 2) the improved performance of the proposed method over state-of-the-art methods that utilize either relative or pairwise constraints; and 3) the robustness of our method in the presence of noisy constraints, such as those provided by human judgement.

I. INTRODUCTION

Unsupervised clustering can be improved with the aid of side information for the task at hand. In general, side information refers to knowledge beyond instances themselves that can help inferring the underlying instance-to-cluster assignments. One common and useful type of side information has been represented in the form of *instance-level constraints* that expose instance-level relationships.

Previous work has primarily focused on the use of *pairwise constraints* (e.g., [1]–[11]), where a pair of instances is indicated to belong to the same cluster by a Must-Link (ML) constraint or to different clusters by a Cannot-Link (CL) constraint. More recently, various studies [12]–[17] have suggested that domain knowledge can also be incorporated in the form of relative comparisons or *relative constraints*, where each constraint specifies *whether instance x_i is more similar to x_j than to x_k .*

We were motivated to focus on relative constraints for a couple of reasons. First, the labeling (proper identification) of relative constraints by humans appears to be more reliable than that of pairwise constraints. Research in psychology has revealed that people are often inaccurate in making absolute judgments (required for pairwise constraints), but they are more trustworthy when judging comparatively [18]. Consider

one of our applications, where we would like to form clusters of bird song syllables based on spectrogram segments from recorded sounds. Figure 1(a) and 1(b) shows examples of the two types of constraints/questions considered. In the examples, syllable 1 in both figures and syllable 3 in 1(b) are from the same singing pattern and syllable 2 in both figures belongs to a different one. From the figures, it is apparent that making an absolute judgment for the pairwise constraint in 1(a) is more difficult. In contrast, the comparative question for labeling relative constraint in 1(b) is much easier to answer. Second, since each relative constraint includes information about three instances, they tend to be more informative than pairwise constraints (even when several pairwise constraints are considered). This is formally characterized in Section II-A.

In the area of learning from relative constraints, most work uses metric learning approaches [12]–[16]. Such approaches assume that there is an underlying metric that determines the outcome of the similarity comparisons, and the goal is to learn such a metric. The learned metric is often later used for clustering (e.g., via Kmeans or related approaches). In practice, however, we may not have access to an *oracle* metric. Often the constraints are provided in a way that instances from the same class are considered more similar than those from different classes. This paper explicitly considers such scenarios where constraints are provided based on the underlying *class concept*. Unlike the metric-based approaches, we aim to directly infer an optimal clustering of the data using the provided relative comparisons, without requiring explicit metric learning.

Formally, we regard each constraint (x_i, x_j, x_k) as being obtained by asking: *is x_i more similar to x_j than to x_k ,* and the answer is provided by a user/oracle based on the underlying instance clusters. In particular, a *yes* answer is given if x_i and x_j are believed to belong to the same cluster while x_k is believed to be from a different one. Similarly, the answer will be *no* if it is believed that x_i and x_k are in the same cluster which is different from the one containing x_j . Note that for some triplets, it may not be possible to provide a *yes* or *no* answer. For example, if the three instances belong to the same cluster, as shown in figure 1(c); or if each of them belongs to a different cluster, as shown in figure 1(d). Such cases have been largely ignored by prior studies. Here, we allow the user to provide a *don't know* answer (*dnk*) when *yes/no* can not be determined. Such *dnk*'s not only allow for improved labeling flexibility, but also provide useful information about instance clusters that can help improve clustering, as will be demonstrated in Section II-A and the experiments.

In this work, we introduce a discriminative clustering method, DCRC, that learns from relative constraints with *yes*,

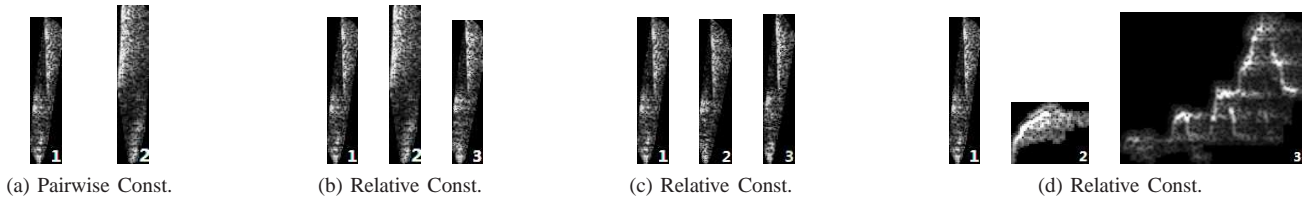


Fig. 1. Examples for labeling pairwise vs. relative constraints from *Birdsong* data. Labeling question for (a): *Do syllable 1 and syllable 2 belong to the same cluster?* Labeling question for (b) (c) and (d): *Is syllable 1 more similar to syllable 2 than to syllable 3?* (a) and (b) reveal the cases where relative constraints are easier to label. The cases in (c) and (d) motivate the introducing of a *don't know* answer for relative constraints.

no, or *dnk* labels (Section III). DCRC uses a probabilistic model that naturally connects the instances, their underlying cluster memberships, and the observed constraints. Based on this model, we present a maximum-likelihood objective with additional terms enforcing cluster separation and cluster balance. Variational EM is used to find approximate solutions (Section IV). In the experiments (Section V), we first evaluate our method on both UCI and additional real-world datasets with simulated noise-free constraints generated from ground-truth class labels. The results demonstrate the usefulness of relative constraints including *don't know* answers, and the performance advantage of our method over current state-of-the-art methods for both relative and pairwise constraints. We also evaluate our method with human-labeled noisy constraints collected from a user study, and results show the superiority of our method over existing methods in terms of robustness to the noisy constraints.

II. PROBLEM ANALYSIS

In this section, we first compare the cluster label information obtained by querying different types of constraints, analyzing the usefulness of relative constraints. Then we formally state the problem.

A. Information from Constraints

Here we provide a qualitative analysis with a simplified but illustrative example. Suppose we have N i.i.d instances $\{x_i\}_{i=1}^N$ sampled from K clusters with even prior $1/K$. Consider a triplet $(x_{t_1}, x_{t_2}, x_{t_3})$ and a pair (x_{b_1}, x_{b_2}) . Let $Y_t = [y_{t_1}, y_{t_2}, y_{t_3}]^T$ and $Y_b = [y_{b_1}, y_{b_2}]^T$ be their corresponding cluster labels. Let $l_t \in \{yes, no, dnk\}$ and $l'_b \in \{ML, CL\}$ be the label for the relative and pairwise constraint respectively. In this example they are determined by

$$l_t = \begin{cases} yes, & \text{if } y_{t_1} = y_{t_2}, y_{t_1} \neq y_{t_3} \\ no, & \text{if } y_{t_1} = y_{t_3}, y_{t_1} \neq y_{t_2} \\ dnk, & o.w. \end{cases} \quad (1)$$

$$l'_b = \begin{cases} ML, & \text{if } y_{b_1} = y_{b_2} \\ CL, & \text{if } y_{b_1} \neq y_{b_2}. \end{cases} \quad (2)$$

We can derive the mutual information between a relative constraint and the associated instance cluster labels as (see Appendix for the derivation)

$$I(Y_t; l_t) = 2 \log K - (1 - P_{dnk}) \log(K - 1) - P_{dnk} \log[K^2 - 2(K - 1)], \quad (3)$$

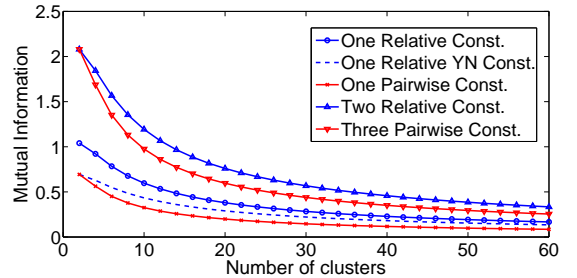


Fig. 2. Mutual information between instance cluster labels and constraint labels as a function of the number of clusters.

and that for a pairwise constraint as

$$I(Y_b; l'_b) = \log K - P_{CL} \log(K - 1), \quad (4)$$

where $P_{dnk} = 1 - 2(K - 1)/K^2$, and $P_{CL} = 1 - 1/K$.

Figure 2 plots the values of (3) and (4) as a function of the number of clusters K . Comparing the values of *one relative const* and *one pairwise const*, we see that, in the absence of other information, a relative constraint provides more information. One might argue that labeling a triplet requires inspecting more instances than labeling a pair, making this comparison unfair. To address this bias, we compare the information gain from the two types of constraints with the same number of instances, namely, comparing the values of *two relative constraints* with that of *three pairwise constraints*, both involving six instances. In Figure 2 we see again that relative constraints are more informative.

Another aspect worth evaluating is the motivation behind explicitly using *dnk* constraints. In prior work on learning from relative constraints, the constraints are typically generated by randomly selecting triplets and producing constraints based their class labels. If a triplet can not be definitely labeled with *yes* or *no*, the resulting constraint is not employed by the learning algorithm (it is ignored). Such methods are by construction not using the information provided by *dnk* answers. However, it is possible to show that in general *dnk*'s can provide information about instance labels. If *dnk*'s are ignored, the mutual information can be computed by replacing $H(Y_t | l_t = dnk)$ with $H(Y_t)$, meaning that the *dnk*'s are not informative about the instance labels. In this case, we have

$$I'(Y_t; l_t) = 2(1 - P_{dnk}) \log K - (1 - P_{dnk}) \log(K - 1). \quad (5)$$

Comparing the values of *one relative YN const* (which ignores

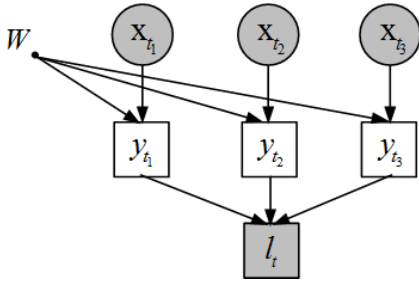


Fig. 3. The dependencies between three instances $(x_{t_1}, x_{t_2}, x_{t_3})$, their cluster labels $(y_{t_1}, y_{t_2}, y_{t_3})$, and the constraint label l_t .

dnk) with that of *one relative const* in Figure 2, we see a clear gap between using and not using *dnk* constraints, implying the informativeness of *dnk* constraints. Additionally, the amount of *dnk* constraints is usually large, especially when the number of clusters is large. Consider randomly selecting triplets from clusters with equal sizes. There is a 50% chance of acquiring *dnk* constraints in two-cluster problems, and the chance increases to 78% in eight-cluster problems. The information provided by such large amount of *dnk* constraints is substantial. Hence, we believe it will be beneficial to explicitly employ and model *dnk* constraints.

B. Problem Statement

Let $X = [x_1, \dots, x_N]^T$ be the given data, where each $x_i \in \mathcal{R}^d$ and d is the feature dimension. Let $Y = [y_1, \dots, y_N]^T$ be the hidden cluster label vector, where y_i is the label of x_i . With slight abuse of notation, we use $\{(t_1, t_2, t_3)\}_{t=1}^M$ to denote the index set of M triplets, representing M relative constraints. Each (t_1, t_2, t_3) contains the indices for the three instances in the t -th constraint. Let $L = [l_1, \dots, l_M]^T$ be the constraint label vector, where $l_t \in \{\text{yes}, \text{no}, \text{dnk}\}$ is the label of $(x_{t_1}, x_{t_2}, x_{t_3})$. Each l_t specifies the answer to the question: *is x_{t_1} more similar to x_{t_2} than to x_{t_3} ?* Our goal is to *partition the data into K clusters such that similar instances are assigned to the same cluster, while respecting the given constraints*. In this paper, we assume that K is pre-specified.

In the following, we will use $I_t = \{t_1, t_2, t_3\}$ to denote the set of indices in the t -th triplet, use I to index all the distinct instances involved in the constraints, i.e., $I = \{1 \leq i \leq N : i \in \cup_{t=1}^M I_t\}$, and use U to index the instances that are not in any constraints.

III. METHODOLOGY

In this section, we introduce our probabilistic model and present the proposed objective functions based on this model.

A. The Probabilistic Model

We propose a *Discriminative Clustering* model for *Relative Constraints* (DCRC). Figure 3 shows the proposed probabilistic model defining the dependencies between the input instances $(x_{t_1}, x_{t_2}, x_{t_3})$, their cluster labels $(y_{t_1}, y_{t_2}, y_{t_3})$, and the constraint label l_t for only one relative constraint. For

TABLE I. DISTRIBUTION OF $P(l_t|Y_t)$, $Y_t = [y_{t_1}, y_{t_2}, y_{t_3}]$.

Cases	$l_t = \text{yes}$	$l_t = \text{no}$	$l_t = \text{dnk}$
$y_{t_1} = y_{t_2}, y_{t_1} \neq y_{t_3}$	$1 - \epsilon$	$\epsilon/2$	$\epsilon/2$
$y_{t_1} = y_{t_3}, y_{t_1} \neq y_{t_2}$	$\epsilon/2$	$1 - \epsilon$	$\epsilon/2$
o.w.	$\epsilon/2$	$\epsilon/2$	$1 - \epsilon$

a collection of constraints, it is possible to have y variables connected to more than one (or none) constraint label l if some instances appear in multiple constraints (or do not appear in any given constraint).

We use a multi-class logistic classifier to model the conditional probability of y 's given the observed x 's. For simplicity, in the following we will use the same notation x to represent the $(d+1)$ -dimensional augmented vector $[x^T, 1]^T$. Let $W = [w_1, \dots, w_K]^T$ be a weight matrix in $\mathcal{R}^{K \times (d+1)}$, where each w_k contains weights on the d -dimensional feature space and an additional bias term. Then the conditional probability is represented as

$$P(y = k|x; W) = \frac{\exp(w_k^T x)}{\sum_{k'} \exp(w_{k'}^T x)}. \quad (6)$$

In our model, the observed constraint labels only depend on the cluster labels of the associated instances. In an ideal scenario, the conditional distribution of l_t given the cluster labels would be deterministic, as described by Eq. (1). However, in practice users can make mistakes and be inconsistent during the annotation process. We address this by relaxing the deterministic relationship to the distribution $P(l_t|Y_t)$ described in Table I. The relaxation is parameterized by $\epsilon \in [0, 1]$, indicating the probability of an error when answering the query. Here we let the two erroneous answers have equal probability $\epsilon/2$. Namely, the ideal label of l_t (e.g., $l_t = \text{yes}$ if $y_{t_1} = y_{t_2}, y_{t_1} \neq y_{t_3}$) is given with probability $1 - \epsilon$, and any other labels (*no* and *dnk* in this case) are given with equal probability $\epsilon/2$. In practice, lower values of ϵ are expected when constraints have fewer noise. Alternatively, we can view this relaxation as allowing the constraints to be *soft* as needed, balancing the trade-off between finding large separation margins among clusters and satisfying all the constraints.

B. Objective

The first part of our objective is to maximize the likelihood of the observed constraints given the instances, i.e.,

$$\begin{aligned} \max_W \Phi(L|X_I; W) &= \frac{1}{M} \log P(L|X_I; W) \\ &= \frac{1}{M} \log \sum_{Y_I} P(L, Y_I|X_I; W), \end{aligned} \quad (7)$$

where I indexes the constrained instances as defined in Section II-B, and $\frac{1}{M}$ is a normalization constant.

To reduce overfitting, we add the standard L-2 regularization for the logistic model, namely,

$$R(W) = \sum_k \tilde{w}_k^T \tilde{w}_k,$$

where each \tilde{w}_k is a vector obtained by replacing the bias term in w_k with 0.

In addition to satisfying the constraints, we also expect the clustering solution to separate the clusters with large margins. This objective can be captured by minimizing the conditional entropy of instance cluster labels given the observed features [19]. Since the cluster information about constrained instances is captured by Eq. (7), we only impose such entropy minimization on the unconstrained instances, i.e.,

$$H(Y_U|X_U; W) = \frac{1}{|U|} \sum_{i \in U} H[P(y_i|x_i; W)] .$$

Adding the above terms together, our objective is

$$\max_W \Phi(L|X_I; W) - \tau H(Y_U|X_U; W) - \lambda R(W) . \quad (8)$$

In some cases, we may also wish to maintain a balanced distribution across different clusters. This can be achieved by maximizing the entropy of the estimated marginal distribution of cluster labels [20], i.e.,

$$H(\hat{y}|X; W) = - \sum_{k=1}^K \hat{p}_k \log \hat{p}_k ,$$

where we denote the estimated marginal probability as $\hat{p}_k = \hat{P}(y = k|X; W) = \frac{1}{N} \sum_{i=1}^N p_{ik}$ and $p_{ik} = P(y_i = k|x_i; W)$.

In cases where balanced clusters are desired, our objective is formulated as

$$\max_W \Phi(L|X_I; W) - \lambda R(W) + \tau [H(\hat{y}|X; W) - H(Y_U|X_U; W)] , \quad (9)$$

where we use the same coefficient τ to control the enforcement of the cluster separation and cluster balance terms, since they are roughly at the same scale.

The two objectives (8) and (9) are non-concave, and optimization generally can only be guaranteed to reach a local optimum. In the next section, we present a variational EM solution and discuss an effective initialization strategy.

IV. OPTIMIZATION

Here we consider optimizing the objective in Eq. (9), which enforces cluster balance. The objective (8) is simpler and can be optimized following the same procedure by simply removing the corresponding terms employed for cluster balance.

Computing the log-likelihood Eq. (7) requires marginalizing over hidden variables Y_I . Exact inference may be feasible when the constraints are highly separated or the number of constraints is small, as this may produce a graphical model with low tree-width. As more y 's are related to each other via constraints, marginalization becomes more expensive to compute, and it is in general intractable. For this reason, we use the variational EM algorithm for optimization.

Applying Jensen's inequality, we obtain the lower bound of the objective as follows

$$LB = \frac{1}{M} E_{Q(Y_I)} \left[\log \left(\frac{P(Y_I, L|X_I; W)}{Q(Y_I)} \right) \right] - \lambda R(W) + \tau [H(\hat{y}|X; W) - H(Y_U|X_U; W)] , \quad (10)$$

TABLE II. THE VALUES OF $\tilde{Q}(l_t|y_i = k)$, $i \in I_t$. FOR SIMPLICITY, WE DENOTE $q_{jk} \equiv q(y_{t_j} = k)$ AND $q_{j\bar{k}} \equiv q(y_{t_j} \neq k)$.

Cases	$l_t = yes$	$l_t = no$	$l_t = dnk$
$i = t_1$	$q_{2k}q_{3\bar{k}}$	$q_{2\bar{k}}q_{3k}$	$1 - q_{2k}q_{3\bar{k}} - q_{2\bar{k}}q_{3k}$
$i = t_2$	$q_{1k}q_{3\bar{k}}$	$\sum_{u \neq k} q_{1u}q_{3u}$	$1 - q_{1k}q_{3\bar{k}} - \sum_{u \neq k} q_{1u}q_{3u}$
$i = t_3$	$\sum_{u \neq k} q_{1u}q_{2u}$	$q_{1k}q_{2\bar{k}}$	$1 - q_{1k}q_{2\bar{k}} - \sum_{u \neq k} q_{1u}q_{2u}$

where $Q(Y_I)$ is a variational distribution. In variational EM, such lower bound is maximized alternately in the E-step and M-step respectively [21]. In each E-step, we aim to find a tractable distribution $Q(Y_I)$ such that the Kullback-Leibler divergence between $Q(Y_I)$ and the posterior distribution $P(Y_I|L, X_I; W)$ is minimized. Given the current $Q(Y_I)$, each M-step finds the new W that maximizes the LB. Note that in the objective (and the LB), only the likelihood term is relevant to the E-step. The other terms are only used in solving for W in the M-steps.

A. Variational E-Step

We use mean field inference [22], [23] to approximate the posterior distribution in part due to its ease of implementation and convergence properties [24]. Mean field restricts the variational distribution $Q(Y_I)$ to the tractable fully-factorized family $Q(Y_I) = \prod_{i \in I} q(y_i)$, and finds the $Q(Y_I)$ that minimizes the KL-divergence $KL[Q(Y_I)||P(Y_I|L, X_I; W)]$. The optimal $Q(Y_I)$ is obtained by iteratively updating each $q(y_i)$ until $Q(Y_I)$ converges. The update equation is

$$q(y_i) = \frac{1}{Z} \exp\{E_{Q(Y_{I \setminus i})}[\log P(X_I, Y_I, L)]\} , \quad (11)$$

where $Q(Y_{I \setminus i}) = \prod_{j \in I, j \neq i} q(y_j)$, and Z is a normalization factor to ensure $\sum_{y_i} q(y_i) = 1$. In the following, we derive a closed-form update for this optimization problem.

Applying the model independence assumptions, the expectation term in Eq. (11) is simplified to

$$E_{Q(Y_{I \setminus i})} \left[\sum_{t=1}^M \log P(l_t|Y_t) + \sum_{j \in I} \log P(y_j|x_j; W) + \log P(X_I) \right] = \sum_{t: i \in I_t} E_{Q(Y_{I_t \setminus i})} [\log P(l_t|Y_t)] + \log P(y_i|x_i; W) + const, \quad (12)$$

where $I_t \setminus i$ is the set of indices in I_t except for i , and $const$ absorbs all the terms that are constant with respect to y_i . The first term in (12) sums over the expected log-likelihood of observing each l_t given the fixed y_i . To compute the expectation, we first let $\tilde{Q}(l_t|y_i)$ be the probability that the observed l_t is consistent with the Y_t given a fixed y_i . That is, $\tilde{Q}(l_t|y_i)$ is the probability for all possible assignments of Y_t given a fixed y_i , such that $P(l_t|Y_t) = 1 - \epsilon$ according to Table I. The $\tilde{Q}(l_t|y_i)$ can be computed straightforwardly as in Table II. Then each of the expectations in (12) is computed as

$$E[\log P(l_t|y_i)] = [1 - \tilde{Q}(l_t|y_i)] \log \frac{\epsilon}{2} + \tilde{Q}(l_t|y_i) \log(1 - \epsilon).$$

From the above, the update Eq. (11) is derived as

$$q(y_i) = \frac{\alpha^{F(y_i)} P(y_i|x_i; W)}{\sum_{y_i} \alpha^{F(y_i)} P(y_i|x_i; W)}, \quad \text{with } \alpha = \frac{2(1-\epsilon)}{\epsilon}, \quad (13)$$

where $F(y_i) = \sum_{l_i: i \in I_i} \tilde{Q}(l_i|y_i)$.

The term $F(y_i)$ can be interpreted as measuring the compatibility of each assignment of y_i with respect to the constraints and the other y 's. In Eq. (13), α is controlled by the parameter ϵ . When $\epsilon \in (0, \frac{2}{3})$, $\alpha > 1$ and the update allows more compatible assignments of y_i , i.e., the ones with higher $F(y_i)$, to have larger $q(y_i)$. When $\epsilon = \frac{2}{3}$, the constraint labels are regarded as uniformly distributed regardless of the instance cluster labels, as can be seen from Table I. In this case, $\alpha = 1$ and each $q(y_i)$ is directly set to the conditional probability $P(y_i|x_i; W)$. This naturally reduces our method to learning without constraints. Clearly, when ϵ is smaller, the constraints are harder and the updates will push $q(y_i)$ to more extreme distributions. Note that the values of $\epsilon \in (\frac{2}{3}, 1)$ cause $\alpha < 1$, which will lead to results that contradict the constraints, and are generally not desired.

Special Case: Hard Constraints. In the special case where $\epsilon = 0$ and $\alpha = \infty$, $P(l_i|Y_i)$ essentially reduces to the deterministic model described in Eq. (1), allowing our model to incorporate *hard* constraints. The update equation of this case can also be addressed similarly to Eq. (13). In this case, $q(y_i)$ is non-zero only when the value of $F(y_i)$ is the maximum among all possible assignments of y_i . Thus, the update equation is reduced to a max model. More formally, we define the max-compatible label set for each instance x_i as

$$Y_i = \{1 \leq k \leq K : F(y_i = k) \geq F(y_i = k'), \forall k' \neq k\}.$$

Namely, each Y_i contains the most compatible assignments for y_i with respect to the constraints. Then the update equation becomes

$$q(y_i) = \begin{cases} \frac{P(y_i|x_i; W)}{\sum_{y'_i \in Y_i} P(y'_i|x_i; W)}, & \text{if } y_i \in Y_i, \\ 0, & \text{o.w.} \end{cases} \quad (14)$$

B. M-Step

The M-step searches for the parameter W that maximizes the *LB*. Applying the independence assumptions again and ignoring all the terms that are constant with respect to W , we obtain the following objective

$$\begin{aligned} \max_W J = & \frac{1}{M} \sum_{Y_I} Q(Y_I) \log P(Y_I|X_I; W) - \lambda R(W) \\ & + \tau [H(\hat{y}|X; W) - H(Y_U|X_U; W)]. \end{aligned}$$

This objective is non-concave and a local optimum can be found via gradient ascent. We used L-BFGS [25] in our experiments. The derivative of J w.r.t. W is

$$\begin{aligned} \frac{\partial J}{\partial W} = & \frac{1}{M} \sum_{i \in I} (Q_i - P_i) x_i^T - 2\lambda \tilde{W} \\ & + \frac{\tau}{|U|} \sum_{j \in U} \sum_k (\mathbf{1}_k - P_j) p_{jk} \log p_{jk} x_j^T \\ & - \frac{\tau}{N} \sum_{n=1}^N \sum_k (\mathbf{1}_k - P_n) p_{nk} \log \hat{p}_{nk} x_n^T, \end{aligned}$$

where $P_i = [p_{i1}, \dots, p_{iK}]^T$, $Q_i = [q_{i1}, \dots, q_{iK}]^T$ with $q_{ik} = q(y_i = k)$, $W = [\tilde{w}_1, \dots, \tilde{w}_K]^T$, and $\mathbf{1}_k$ is a K -dimensional vector that contains the value 1 on the k -th dimension and 0 elsewhere.

The above derivations use a linear model for $P(y|x; W)$, and thus the learned DCRC is also linear. However, all of the results can be easily generalized to using kernel functions, allowing DCRC to find non-linear separation boundaries.

C. Complexity and Initialization

In each E-step, the complexity is $\mathcal{O}(\gamma K |I|)$, where γ is the number of mean-field iterations for $Q(Y_I)$ to converge. In the M-step, the complexity of computing the gradient of W in each L-BFGS iteration is $\mathcal{O}(NKD)$.

Although mean-field approximation is guaranteed to converge, in the first few E-steps it is not critical to achieve a very close approximation. In practice, we can run mean-field update up to a fixed number of iterations (e.g., 100). We empirically observe that the approximation still converges very fast in later EM iterations. Similarly, we observe in the M-step that the L-BFGS optimization usually converges with very few iterations in the later EM runs, and a completion of a fixed number of iterations for L-BFGS is also sufficient in the first few M-steps.

The EM algorithm is generally sensitive to the initial parameter values. Here we first apply Kmeans and train a supervised logistic classifier with the clustering results. The learned weights are then used as the starting point of DCRC. Empirically we observe that such initialization typically allows DCRC to converge within 100 iterations.

V. EXPERIMENTS

In this section, we experimentally examine the effectiveness of our model in utilizing relative constraints to improve clustering. We first evaluate all methods on both UCI and other real-world datasets with noise-free constraints generated from true class labels. We then present a preliminary user study where we ask users to label constraints and evaluate all the methods on these human-labeled (noisy) constraints.

A. Baseline Methods and Evaluation Metric

We compare our algorithm with existing methods that consider relative constraints or pairwise constraints. The methods employing pairwise constraints are *Xing's* method [2] (distance metric learning for a diagonal matrix) and *ITML* [26]. These are the state-of-the-art methods that are usually compared in the literature and have publicly available source code.

For methods considering relative constraints, we compare with: 1) *LSML* [15], a very recent metric learning method studying relative constraints (we use Euclidean distance as the prior); 2) *SSSVaD* [16], a method that directly finds clustering solutions with relative constraints; and 3) *sparseLP* [13], an earlier method that hasn't been extensively compared. We also experimented with a SVM-style method proposed in [12] and observed that its performance is generally worse. Thus, we do not report the results on this method.

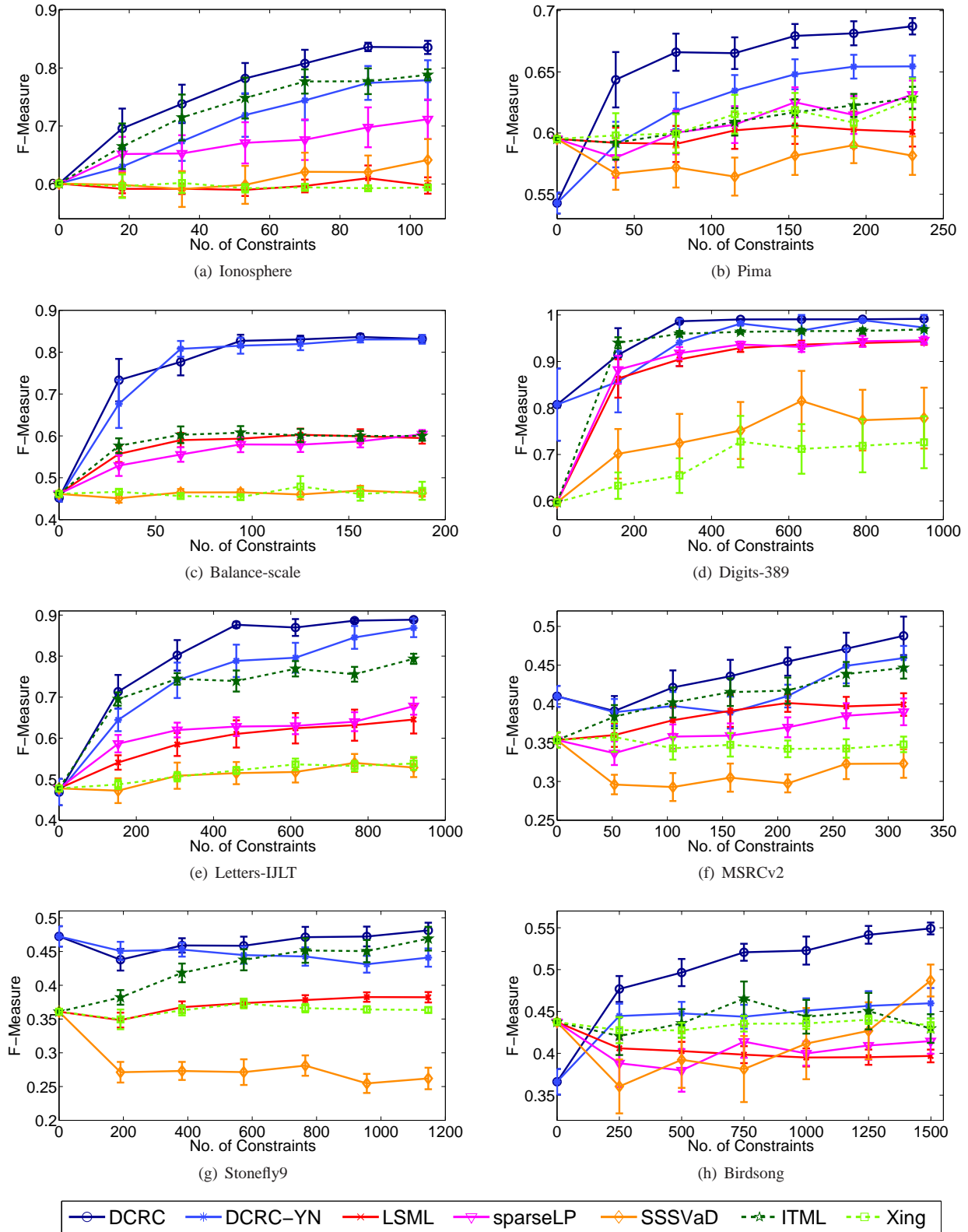


Fig. 4. (Best viewed in color.) The F-measure as a function of number of relative constraints. Results are averaged over 20 runs with independently sampled constraints. Error bars are shown as 95% confidence intervals.

TABLE III. SUMMARY OF DATASET INFORMATION

Dataset	#Inst.	#Dim.	#Cluster
Ionosphere	351	34	2
Pima	768	8	2
Balance-scale	625	4	3
Digits-389	3165	16	3
Letters-IJLT	3059	16	4
MSRCv2	1046	48	6
Stonefly9	3824	285	9
Birdsong	4998	38	13

Xing’s method, ITML, LSML, and sparseLP are metric learning techniques. Here we apply Kmeans with the learned metric (50 times) to form cluster assignments, and the clustering solution with the minimum mean-squared error is chosen.

We evaluated the clustering results based on the ground-truth class labels using *pairwise F-measure* [3], *Adjusted Rand Index* and *Normalized Mutual Information*. The results are highly similar with different measures, thus we only present the F-Measure results.

B. Controlled Experiments

In this set of experiments, we use simulated noise-free constraints to evaluate all the methods.

1) *Datasets*: We evaluate all methods on five UCI datasets: *Ionosphere*, *Pima*, *Balance-Scale*, *Digits-389*, and *Letters-IJLT*. We also use three extra real-world datasets: 1) a subset of image segments of the *MSRCv2* data¹, which contains the six largest classes of the image segments; 2) the HJA *Birdsong* data [27], which contains automatically extracted segments from spectrograms of birdsong recordings, and the goal is to identify the species for each segment; and 3) the *Stonefly9* data [28], which contains insect images and the task is to identify the species of the insect for each image. Table III summarizes the dataset information. In our experiments, all features are standardized to have zero mean and unit standard deviation.

2) *Experimental Setup*: For each dataset, we vary the number of constraints from $0.05N$ to $0.3N$ with a $0.05N$ increment, where N is the total number of instances. For each size, triplets are randomly generated and constraint labels are assigned according to Eq. (1). We evaluated our method in two settings, one with all constraints as input (shown as *DCRC*), and the other with only *yes/no* constraints (shown as *DCRC-YN*). The baseline methods for relative constraints are designed for *yes/no* constraints only and cannot be easily extended to incorporate *dnk* constraints, so we drop the *dnk* constraints for these methods. To form the corresponding pairwise constraints, we infer one ML and one CL constraints from each relative constraint with *yes/no* labels (note that no pairwise constraints could be directly inferred from *dnk* relative constraints). Thus, all the baselines use the same information as *DCRC-YN*, since no *dnk* constraints are employed by them.

We use five-fold cross-validation to tune parameters for all methods. The same training and validation folds are used across all the methods (removing *dnk* constraints, or converting to pairwise constraints when necessary). For each method,

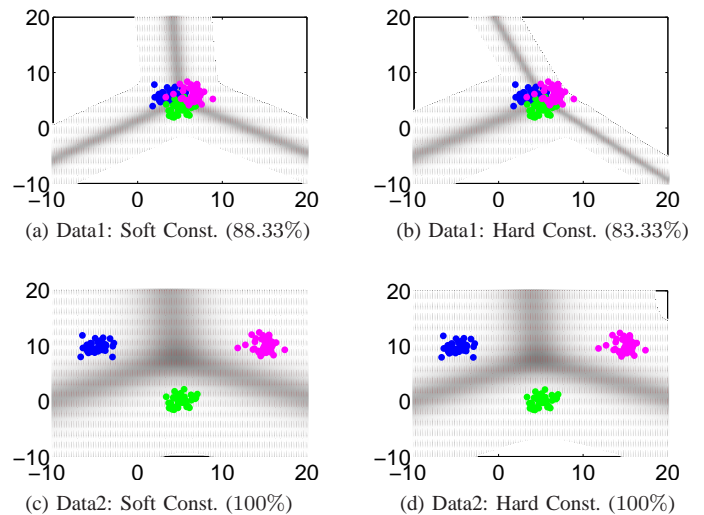


Fig. 5. Estimated entropy using soft/hard constraints on synthetic datasets. Cluster assignments are represented with blue, pink, and green points. Entropy regions are shaded, with darker color representing higher entropy. Prediction accuracy on instance cluster labels is shown in the parentheses.

we select the parameters that maximize the averaged constraint prediction accuracy on the validation sets. For our method, we search for the optimal $\tau \in \{0.5, 1, 1.5\}$ and $\lambda \in \{2^{-10}, 2^{-8}, 2^{-6}, 2^{-4}, 2^{-2}\}$. We empirically observed that our method is very robust to the choice of ϵ when it is within the range $[0.05, 0.15]$. Here we set $\epsilon = 0.05$ for this set experiments with the simulated noise-free constraints. Experiments are repeated using 20 randomized runs, each with independently sampled constraints.

3) *Overall Performance*: Figure 4 shows the performance of all methods with different number of constraints. The sparseLP does not scale to the high-dimensional *Stonefly9* dataset and hence is not reported on this particular data.

From the results we see that *DCRC* consistently outperforms all baselines on all datasets as the constraints increase, demonstrating the effectiveness of our method.

Comparing *DCRC* with *DCRC-YN*, we observe that the additional *dnk* constraints provide substantial benefits, especially for datasets with large number of clusters (e.g., *MSRCv2*, *Birdsong*). This is consistent with our expectation because the portion of *dnk* constraints increases significantly when K is large, leading to more information to be utilized by *DCRC*.

Comparing *DCRC-YN* with the baselines, we observe that *DCRC-YN* achieves comparable or better performance even compared with the best baseline *ITML*. This suggests that, with noise-free constraints, our model is competitive with the state-of-the-art methods even without considering the additional information provided by *dnk* constraints.

4) *Soft Constraints vs. Hard Constraints*: In this set of experiments, we explore the impact on our model when soft constraints ($\epsilon = 0.05$) and hard constraints ($\epsilon = 0$) are used respectively. We first use two synthetic datasets to examine and illustrate their different behaviors. These two datasets each contain three clusters, 50 instances per cluster. The clusters are close to each other in one dataset, and far apart

¹<http://research.microsoft.com/en-us/projects/ObjectClassRecognition/>

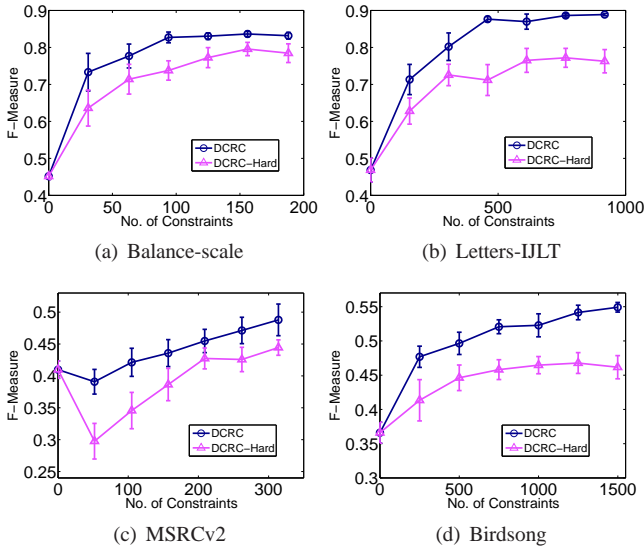


Fig. 6. Performance of DCRC using soft constraints vs. hard constraints.

(and thus easily separable) in the other. For each dataset, we randomly generated 500 relative constraints using points near the decision boundaries. Figure 5 shows the prediction entropy and prediction accuracy on instances cluster labels for both datasets achieved by our model, using soft and hard constraints respectively. We can see that when clusters are easily separable, both soft and hard constraints produce reasonable decision boundaries and perfect prediction accuracy. However, when cluster boundaries are fuzzy, the results of using soft constraints appear preferable. This indicates that by *softening* the constraints, our method could search for more reasonable decision to avoid overfitting to the constrained instances.

We then compare the performances of using soft ($\epsilon = 0.05$) versus hard ($\epsilon = 0$) constraints on real datasets with the same setting utilized in Section V-B3. Due to space limit, here we only show results on four representative datasets in Figure 6. The behavior of other datasets are similar. We can see that using soft constraints generally leads to better performance than using hard constraints. In particular, on the *MSRCv2* dataset, using hard constraints produces a large “dip” at the beginning of the curve while this issue is not severe for soft constraints. This suggests that using soft constraints makes our model less susceptible to overfitting to small sets of constraints.

5) *Effect of Cluster Balance Enforcement*: This set of experiments test the effect of the cluster balance enforcement on the performance of DCRC for the unbalanced *Birdsong* and the balanced *Letters-IJLT* datasets. Figure 7 reports the performance of DCRC (soft constraints, $\epsilon = 0.05$) with and without such enforcement with varied number of constraints. We see that when there is no constraint, it is generally beneficial to enforce the cluster balance. The reason is, when cluster balance is not enforced, the entropy that enforces cluster separation can be trivially reduced by removing cluster boundaries, causing degenerate solutions. However, as the constraint increases, enforcing cluster balance on the unbalanced *Birdsong* hurts

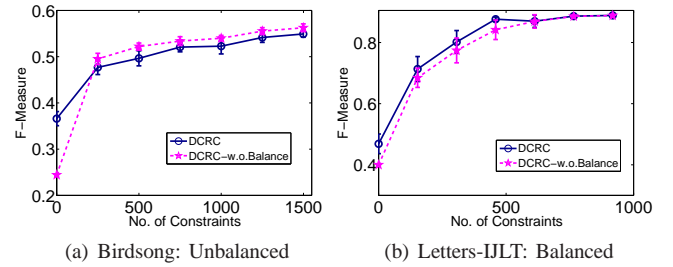


Fig. 7. Performance of DCRC with/without cluster balance enforcement.

the performance. Conceivably, such enforcement would cause DCRC to prefer solutions with balanced cluster distributions, which is undesirable for datasets with uneven classes. On the other hand, appropriate enforcement on the balanced *Letters-IJLT* dataset provides further improvement. In practice, one could determine whether to enforce cluster balance based on prior knowledge of the application domain.

6) *Computational Time*: We record the runtime of learning with 1500 constraints on the *Birdsong* dataset, on a standard desktop computer with 3.4 GHz CPU and 11.6 GB of memory. On average it takes less than 2 minutes to train the model using an un-optimized Matlab implementation. This is reasonable for most applications with similar scale.

C. Case Study: Human-labeled Constraints

We now present a case study where we investigate the impact of human-labeled constraints on the proposed method and its competitors.

1) *Dataset and Setup*: This case study is situated in one of our applications where the goal is to find bird singing patterns by clustering. The birdsong dataset used in Section V-B contains spectrogram segments labeled with bird species. In reality, birds of the same species may vocalize in different patterns, which we hope to identify as different clusters. Toward this goal, we created another birdsong dataset consisting of clusters that contains relatively pure singing patterns. We briefly describe the data generation process as follows.

We first manually selected a collection of representative examples of the singing patterns, and then use them as templates to extract segments from birdsong spectrograms by applying template matching. Each of the extracted segments is assigned to the cluster represented by the corresponding template. We then manually inspected and edited the clusters to ensure the quality of the clusters. As a result, each cluster contains relatively pure segments that are actually from the same bird species and represent the same vocalization pattern. See Figure 1 for examples of several different vocalization patterns, which we refer to as syllables. We extract features for each segment using the same method as described in [27]. This process results in a new *Birdsong* dataset containing 2601 instances and 14 ground-truth clusters.

After obtaining informed consents according to the protocol approved by the Institutional Review Board of our institution, we tested six human subjects’ behaviors on labeling constraints. None of the users has any prior experience/knowledge

TABLE IV. THE AVERAGE CONFUSION MATRIX OF THE HUMAN LABELED CONSTRAINTS VS. THE CONSTRAINT LABELS INFERRED FROM TRUE INSTANCE CLUSTERS.

(a) Relative Constraints				(b) Pairwise Constraints		
True	Human Labels			True	Human Labels	
	<i>yes</i>	<i>no</i>	<i>dnk</i>		<i>ML</i>	<i>CL</i>
<i>yes</i>	18.50	0.33	4.83	<i>ML</i>	42.50	9.67
<i>no</i>	0.33	16.50	4.50	<i>CL</i>	10.83	162.00
<i>dnk</i>	3.50	3.00	98.50			

TABLE V. F-MEASURE PERFORMANCE (MEAN \pm STD) WITH THE HUMAN LABELED CONSTRAINTS.

(a) Without using constraints		(b) Using 150 relative constraints	
Method	F-Measure	Method	F-Measure
DCRC-NoConst	0.5175 \pm 0.0232	DCRC	0.7620 \pm 0.1335
Kmeans	0.6523 \pm 0.0189	DCRC-YN	0.7635 \pm 0.1067
		LSML	0.6409 \pm 0.0654
		sparseLP	0.5200 \pm 0.0706
		SSSVaD	0.6046 \pm 0.0605

(c) Using 150 pairwise constraints		(d) Using 225 pairwise constraints	
Method	F-Measure	Method	F-Measure
ITML	0.6409 \pm 0.0424	ITML	0.6347 \pm 0.0372
Xing	0.6438 \pm 0.0423	Xing	0.6438 \pm 0.0282

on the data. They were first given a short tutorial on the data and the concepts of *clustering* and *constraints*. Then each user is asked to label randomly selected 150 triplets, and 225 pairs, using a graphical interface that displays the spectrogram segments. To neutralize the potential bias introduced by the task ordering (triplets vs. pairs), we randomly split the users into two groups with each group using a different ordering.

2) *Results and Discussion*: Table IV lists the average confusion matrix of the human-labeled constraints versus the labels produced based on the ground-truth cluster labels. From Table IV(a), we see that the *dnk* constraints make up more than half of the relative constraints, which is consistent with our analysis in Section II-A that the number of *dnk* constraints can be dominantly large. The users rarely confuse between the *yes* and *no* labels but they do tend to provide more erroneous *dnk* labels. This phenomenon is not surprising because when in doubt, we are often more comfortable to abstain from giving a definite *yes/no* answer and resort to the *dnk* option.

For pairwise constraints, the *CL* constraints are the majority, and the confusions for both *CL* and *ML* are similar. We note that the confusion between the *yes/no* constraints is much smaller than that of *ML/CL* constraints. This shows that the increased flexibility introduced by *dnk* label allows the users to more accurately differentiate *yes/no* labels. The overall labeling accuracy of pairwise constraints is slightly higher than that of relative constraints. We suspect that this is due to the presence of the large amount of *dnk* constraints.

We evaluated all the methods using these human-labeled constraints. To account for the labeling noise in the constraints, we set $\epsilon = 0.15$ for DCRC and DCRC-YN². The averaged results for all methods are listed in Table V. We observe that while most of the competing methods' performance degrade

with added constraints compared with unsupervised Kmeans, our method still shows significant performance improvement even with the noisy constraints. We want to point out that the performance difference we observe is not due to the use of the multi-class logistic classifier. In particular, as shown in Table V(a), without considering any constraints, the logistic model achieves significantly lower performance than Kmeans. This further demonstrates the effectiveness of our method in utilizing the side information provided by noisy constraints to improve clustering.

Recall that ITML is competitive with DCRC-YN previously considering noise-free constraints. Here with noisy constraints, DCRC-YN achieves far better accuracy than ITML, suggesting that our method is much more robust to labeling noise. It is also worth noting that although the *dnk* constraints tend to be quite noisy, they do not seem to degrade the performance of DCRC compared with DCRC-YN.

Our case study also points to possible ways to further improve our model. As revealed by Table IV, the noise on the labels for relative constraints is not uniform as assumed by our model. An interesting future direction is to introduce a non-uniform noise process to more realistically model the users' labeling behaviors.

VI. RELATED WORK

Clustering with Constraints: Various techniques have been proposed for clustering with pairwise constraints [4]–[8], [10]. Our work is aligned with most of these methods in the sense that we assume the guidance for labeling constraints is the underlying instance clusters.

Fewer work has been done on clustering with relative constraints. The work in [12]–[16] propose metric learning approaches that use $d(x_i, x_j) < d(x_i, x_k)$ to encode that x_i is more similar to x_j than to x_k , where $d(\cdot)$ is the distance function. The work [15] studies learning from relative comparisons between two pairs of instances, which can be viewed as the same type of constraints when only three distinct examples are involved. By construction, these methods only consider constraints with *yes/no* labels. Practically, such answers might not always be provided, causing limitation of their applications. In contrast, our method is more flexible by allowing users to provide *dnk* constraints,

There also exist studies that encode the instance relative similarities in the form of hierarchical ordering and attempt hierarchical algorithms that directly find clustering solutions satisfying the constraints [17], [29]. Different with those studies, our work builds on a natural probabilistic model that has not been considered for learning with relative constraints.

Semi-supervised Learning: Related work also exists in a much broader area of semi-supervised learning, involving studies on both clustering and classification problems. The work [19] proposes that to enforce the formed clusters with large separation margins, we could minimize the entropy on the unlabeled data, in addition to learning from the labeled ones. The study [20] suggests to also maximize the entropy of the cluster label distribution in order to find balanced clustering solution. Our final formulation draws inspiration from the above work.

²For these noisy constraints, our method remains robust to the choice of ϵ . Using different values of ϵ ranging from 0.05 to 0.2 only introduces minor fluctuations (within 0.01 difference) to the F-measure.

VII. CONCLUSIONS

In this paper, we studied clustering with relative constraints, where each constraint is generated by posing a query: *is x_i more similar to x_j than to x_k* . Unlike existing methods that only consider *yes/no* responses to such queries, we studied the case where the answer could also be *dnk* (don't know). We developed a probabilistic method DCRC that learns to cluster the instances based on the responses acquired by such queries. We empirically evaluated the proposed method using both simulated (noise-free) constraints and human-labeled (noisy) constraints. The results demonstrated the usefulness of *dnk* constraints, the significantly improved performance of DCRC over existing methods, and the superiority of our method in terms of the robustness to noisy constraints.

REFERENCES

- [1] K. Wagstaff, C. Cardie, S. Rogers, and S. Schrödl, "Constrained K-means Clustering with Background Knowledge," in *ICML*, 2001, pp. 577–584.
- [2] E. Xing, A. Ng, M. Jordan, and S. Russell, "Distance Metric Learning with Application to Clustering with Side-information," in *NIPS*, 2003, pp. 521–528.
- [3] M. Bilenko, S. Basu, and R. J. Mooney, "Integrating Constraints and Metric Learning in Semi-supervised Clustering," in *ICML*, 2004.
- [4] N. Shental, A. Bar-hillel, T. Hertz, and D. Weinshall, "Computing Gaussian Mixture Models with EM using Equivalence Constraints," in *NIPS*, 2003.
- [5] Z. Lu and T. K. Leen, "Semi-supervised Learning with Penalized Probabilistic Clustering," in *NIPS*, 2004.
- [6] S. Basu, M. Bilenko, and R. J. Mooney, "A Probabilistic Framework for Semi-supervised Clustering," in *KDD*, 2004, pp. 59–68.
- [7] T. Lange, M. H. C. Law, A. K. Jain, and J. M. Buhmann, "Learning with Constrained and Unlabelled Data," in *CVPR*, 2005, pp. 731–738.
- [8] B. Nelson and I. Cohen, "Revisiting Probabilistic Models for Clustering with Pair-wise Constraints," in *ICML*, 2007, pp. 673–680.
- [9] R. Ge, M. Ester, W. Jin, and I. Davidson, "Constraint-Driven Clustering," in *KDD*, 2007, pp. 320–329.
- [10] Z. Lu, "Semi-supervised Clustering with Pairwise Constraints: A Discriminative Approach," *Journal of Machine Learning Research*, vol. 2, pp. 299–306, 2007.
- [11] S. Basu, I. Davidson, and K. Wagstaff, *Constrained Clustering: Advances in Algorithms, Theory, and Applications*, 1st ed. Chapman & Hall/CRC, 2008.
- [12] M. Schultz and T. Joachims, "Learning a Distance Metric from Relative Comparisons," in *NIPS*, 2003, p. 41.
- [13] R. Rosales and G. Fung, "Learning Sparse Metrics via Linear Programming," in *KDD*, 2006, pp. 367–373.
- [14] K. Huang, Y. Ying, and C. Campbell, "Generalized Sparse Metric Learning with Relative Comparisons," *Knowl. Inf. Syst.*, vol. 28, no. 1, pp. 25–45, 2011.
- [15] E. Y. Liu, Z. Guo, X. Zhang, V. Jovic, and W. Wang, "Metric Learning from Relative Comparisons by Minimizing Squared Residual," in *ICDM*, 2012, pp. 978–983.
- [16] N. Kumar and K. Kummamuru, "Semisupervised Clustering with Metric Learning using Relative Comparisons," *IEEE Trans. Knowl. Data Eng.*, vol. 20, no. 4, pp. 496–503, 2008.
- [17] E. Liu, Z. Zhang, and W. Wang, "Clustering with Relative Constraints," in *KDD*, 2011, pp. 947–955.
- [18] J. Nunnally and I. Bernstein, *Psychometric Theory*. McGraw Hill, Inc., 1994.
- [19] Y. Grandvalet and Y. Bengio, "Semi-supervised Learning by Entropy Minimization," in *NIPS*, 2005, pp. 33–40.
- [20] R. Gomes, A. Krause, and P. Perona, "Discriminative Clustering by Regularized Information Maximization," in *NIPS*, 2010, pp. 775–783.
- [21] C. M. Bishop, *Pattern Recognition and Machine Learning*, 1st ed. Springer, 2007.
- [22] L. Saul, T. Jaakkola, and M. Jordan, "Mean Field Theory for Sigmoid Belief Networks," *Journal of Artificial Intelligence Research*, vol. 4, pp. 61–76, 1996.
- [23] C. W. Fox and S. J. Roberts, "A tutorial on Variational Bayesian Inference," *Artificial Intelligence Review*, vol. 38, no. 2, pp. 85–95, 2012.
- [24] M. Benaim and J.-Y. L. Boudec, "On Mean Field Convergence and Stationary Regime," *arXiv preprint arXiv:1111.5710*, 2011.
- [25] M. Schmidt, "L-bfgs software," Website, 2012, <http://www.di.ens.fr/~mschmidt/Software/minFunc.html>.
- [26] J. V. Davis, B. Kulis, P. Jain, S. Sra, and I. S. Dhillon, "Information-Theoretic Metric Learning," in *ICML*, 2007, pp. 209–216.
- [27] F. Briggs, X. Z. Fern, and R. Raich, "Rank-loss Support Instance Machines for MIML Instance Annotation," in *KDD*, 2012, pp. 534–542.
- [28] G. Martinez-Munoz, N. Larios, E. Mortensen, W. Zhang, A. Yamamuro, R. Paasch, N. Payet, D. Lytle, L. Shapiro, S. Todorovic, A. Moldenke, and T. Dietterich, "Dictionary-Free Categorization of Very Similar Objects via Stacked Evidence Trees," in *CVPR*, 2009, pp. 549–556.
- [29] K. Bade and A. Nürnberger, "Hierarchical Constraints," *Machine Learning*, pp. 1–29, 2013.

APPENDIX

This appendix provides the derivation of the mutual information Eq. (3). The derivations for Eqns. (4) and (5) are similar and are omitted here.

By definition, the mutual information between the instance labels $Y_t = [y_{t_1}, y_{t_2}, y_{t_3}]$ and the constraint label l_t is

$$I(Y_t; l_t) = H(Y_t) - H(Y_t|l_t). \quad (15)$$

The first entropy term is $H(Y_t) = -\sum_{Y_t} P(Y_t) \log P(Y_t) = 3 \log K$, where we used the independence assumption $P(Y_t) = \prod_{i=1}^3 P(y_{t_i})$ and substituted the prior $P(y_{t_i} = k) = 1/K$. By definition, the second entropy term is

$$H(Y_t|l_t) = -\sum_{a \in \{yes, no, dnk\}} P(l_t = a) \sum_{Y_t} P(Y_t|l_t = a) \log P(Y_t|l_t = a).$$

Now we need to compute the marginal distribution $P(l_t)$ and the conditional distribution $P(Y_t|l_t)$. Based on Eq. (1), the $P(l_t)$ are

$$\begin{aligned} P(l_t = yes) &= \sum_{Y_t} P(Y_t) P(l_t = yes|Y_t) \\ &= \sum_{k=1}^K P(y_{t_1} = k) P(y_{t_2} = k) [1 - P(y_{t_3} = k)] = \frac{K-1}{K^2}. \end{aligned}$$

By distribution symmetry, $P(l_t = no) = P(l_t = yes)$. Then $P(l_t = dnk) = 1 - P(l_t = yes) - P(l_t = no) = 1 - [2(K-1)]/K^2$. To compute $P(Y_t|l_t)$, we notice that for the cluster label assignments that do not satisfy the conditions for the corresponding l_t described in Eq. (1), the probability $P(Y_t|l_t) = 0$. For those satisfying such conditions, the $P(Y_t|l_t)$ are

$$\begin{aligned} P(Y_t|l_t = yes) &= [P(Y_t) P(l_t = yes|Y_t)] / P(l_t = yes) \\ &= [P(Y_t) \times 1] / P(l_t = yes) = \frac{1}{K(K-1)}. \end{aligned}$$

By symmetry again, $P(Y_t|l_t = no) = P(Y_t|l_t = yes)$. Also,

$$\begin{aligned} P(Y_t|l_t = dnk) &= [P(Y_t)P(l_t = dnk|Y_t)]/P(l_t = dnk) \\ &= [P(Y_t) \times 1]/P(l_t = dnk) = \frac{1}{K[K^2 - 2(K-1)]}. \end{aligned}$$

Substituting the values of $P(Y_t|l_t)$ and $P(Y_t)$, we obtain

$$H(Y_t|l_t) = \log K + (1 - P_{dnk}) \log(K-1) + P_{dnk} \log[K^2 - 2(K-1)],$$

where we denote $P_{dnk} = P(l_t = dnk)$.

Substituting $H(Y_t)$ and $H(Y_t|l_t)$ into Eq. (15), we derive

$$I(Y_t; l_t) = 2 \log K - (1 - P_{dnk}) \log(K-1) - P_{dnk} \log[K^2 - 2(K-1)]. \quad \square$$